

Highlights

ALADYN: a set of Anharmonic LAttice DYNamics codes to compute thermodynamic and thermal transport properties of crystalline solids

Keivan Esfarjani, Harold Stokes, Safoura Nayeb Sadeghi, Yuan Liang, Bikash Timalsina, Han Meng, Junichiro Shiomi, Bolin Liao, Ruoshi Sun

- Can extract harmonic and anharmonic force constants up to 8th order, imposing different invariance constraints.
- The state of thermal equilibrium (atomic positions and crystal shape and size) can be predicted at any temperature and volume (or pressure)
- Thermophysical properties such as elastic constants, Gruneisen parameters, free energy, thermal expansion and thermal conductivity from Boltzmann equation (BE) can be predicted from the knowledge of the extracted force constants
- Can also perform molecular dynamics simulations and calculate atomic trajectories and heat current using the extracted anharmonic force field. This is the more accurate alternative to solving BE, as it treats anharmonicity and mass disorder beyond perturbation theory.

ALADYN: a set of Anharmonic Lattice DYNamics codes to compute thermodynamic and thermal transport properties of crystalline solids[★]

Keivan Esfarjani^{a,b}, Harold Stokes^c, Safoura Nayeb Sadeghi^d, Yuan Liang^b, Bikash Timalsina^d, Han Meng^{f,g}, Junichiro Shiomi^{f,g}, Bolin Liao^h and Ruoshi Sunⁱ

^aDept. of Materials Science and Engineering, University of Virginia, Charlottesville, 22904, Virginia, USA

^bDept. of Physics, University of Virginia, Charlottesville, 22904, Virginia, USA

^cDept. of Physics and Astronomy, Brigham Young University, Provo, 84602, Utah, USA

^dDept. of Mechanical and Aerospace Engineering, University of Virginia, Charlottesville, 22904, Virginia, USA

^eDept. of Mechanical Engineering and Materials Science, University of Pittsburgh, Pittsburgh, 15261, Pennsylvania, USA

^fDepartment of Mechanical Engineering, University of Tokyo, 7-3-1 Hongo, Bunkyo, Tokyo, 113-8656, Japan

^gInstitute of Engineering Innovation, University of Tokyo, 2-11-16 Yayoi, Bunkyo, Tokyo, 113-0032, Japan

^hDepartment of Mechanical Engineering, University of California, Santa Barbara, 93106, California, USA

ⁱResearch Computing, University of Virginia, Charlottesville, 22903, Virginia, USA

ARTICLE INFO

Keywords:

Lattice dynamics, anharmonicity, force constants, elastic properties, phonons

ABSTRACT

We introduce a lattice dynamics package which calculates elastic, thermodynamic and thermal transport properties of crystalline materials from data on their force and potential energy as a function of atomic positions. The data can come from density functional theory (DFT) calculations or classical molecular dynamics runs performed in a supercell. First, the model potential parameters, which are anharmonic force constants are extracted from the latter runs. Then, once the anharmonic model is defined, thermal conductivity and equilibrium properties at finite temperatures can be computed using lattice dynamics, Boltzmann transport theories, and a variational principle respectively. In addition, the software calculates the mechanical properties such as elastic tensor, Grüneisen parameters and the thermal expansion coefficient within the quasi-harmonic approximation (QHA). Phonons, elastic constants and thermodynamic properties results applied to the germanium crystal will be illustrated. Using the force constants as a force field, one may also perform molecular dynamics (MD) simulations in order to investigate the combined effects of anharmonicity and defect scattering beyond perturbation theory.

1. Introduction

The theory of lattice dynamics, based essentially on the physics of the harmonic oscillator has shaped the science behind the thermophysical properties of materials. Nowadays, with the advances in computer software and hardware, calculations of the electronic ground state properties of materials, based on the density functional theory has become routine. Total energy and forces on atoms are an output of such theories, and this has allowed us Esfarjani and Stokes (2008) to develop methodologies to compute force derivatives, or force constants (FCs), in order to obtain the parameters of an anharmonic lattice dynamics model. Many softwares are nowadays available to compute force constants of crystalline solids. Among them, we can name ALAMODE Tadano, Gohda, and Tsuneyuki (2014); Tadano and Tsuneyuki (2018), ShengBTE Li, Carrete, Katcho, and Mingo (2014), AlmaBTE Carrete, Vermeersch, Katre, van Roekeghem, Wang, and Madsen (2017), Phonopy Togo and Tanaka (2015), SSCHA Monacelli, Bianco, Cherubini, Calandra, Errea, and Mauri (2021), Hiphive Eriksson, Fransson, and Erhart (2019), TDEP Hellman, Steneteg, Abrikosov, and Simak (2013); Hellman and Abrikosov (2013), Phonon Parlinski, Li, and Kawazoe (1997), Phon Alfè (2009) ... and many others. Here, we are presenting a new set of codes based on our original paper Esfarjani and Stokes (2008) to compute thermophysical properties of anharmonic crystals. These codes are similar in capabilities but different in the way the FCs are extracted and processed. Our code to calculate the thermal

[★]This research project is funded by the National Science Foundation, NSF-CSSI, Office of Advanced Cyberinfrastructure, award number 2103989.

*Corresponding author

ORCID(s): 0000-0003-1969-0956 k1@virginia.edu (K. Esfarjani)

conductivity (THERMACOND) uses full symmetry of the crystal to compute the non-equilibrium distribution function more efficiently. Codes to compute the free energy and the state of equilibrium at high temperatures, as well as the computation of mechanical properties are relatively novel. In addition, we provide codes (ANFOMOD) to perform molecular dynamics simulations and calculate the heat current with the extracted polynomial force field. In what follows, we describe the methodology and capabilities of the code to extract force constants, FOCEX, which stands for FOrcE Constants EXtraction. The FCs are extracted from a set of displacement-force data on atoms in one or many supercells. They can be used as input to the code ANFOMOD (ANharmonic FOrcE MOlecular Dynamics) to perform MD simulations and calculate the heat current and thermal conductivity from the exact Green-Kubo formula, thereby incorporating anharmonicity and defect scattering beyond perturbation theory. Our other codes, which take as input the extracted force constants, compute the thermal conductivity (THERMACOND) and the state of thermal equilibrium, including structural phase changes, at finite temperatures (SCOP8). They will be described in other upcoming papers.

2. The FOrcE Constants EXtraction (FOCEX) code

Let us start by defining the anharmonic lattice dynamics (LD) model potential energy V^{LD} , which is a Taylor expansion of the potential energy of a crystal in powers of atomic displacements measured from a reference (usually a lattice-) position. The model potential energy can be written in the following form:

$$V^{LD} = E_0 + \sum_i \Pi_i u_i + \frac{1}{2!} \sum_{ij} \Phi_{ij} u_i u_j + \frac{1}{3!} \sum_{ijk} \Psi_{ijk} u_i u_j u_k + \frac{1}{4!} \sum_{ijkl} \chi_{ijkl} u_i u_j u_k u_l + \dots \quad (1)$$

where the roman index i labels the triplet (R, τ, α) with R being a translation vector of the primitive lattice, τ refers to an atom within the primitive unit cell, and α is the cartesian coordinate of the atomic displacement u . In other words, u_i is the displacement of the atom (R, τ) in the direction α from its reference position defined by the vector $(R + \tau)$. Φ, Ψ and χ are respectively the harmonic, cubic and quartic FCs, whereas Π is the negative of the residual force on atom i , and is zero if the potential energy V is expanded around its minimum or ground state configuration where (R, τ) are the equilibrium positions of the atoms. Although this is usually the case, i.e. $\Pi_i = 0$, in low-symmetry crystals, this term maybe non-zero but small due to imperfect convergence in atomic relaxations. In clusters or molecules the formalism is the same, only the translation vector R needs to be dropped. The resulting LD model force on atom i would then be

$$F_i^{LD} = -\frac{\partial V}{\partial u_i} = -\Pi_i - \sum_j \Phi_{ij} u_j - \frac{1}{2} \sum_{jk} \Psi_{ijk} u_j u_k - \frac{1}{3!} \sum_{jkl} \chi_{ijkl} u_j u_k u_l + \dots \quad (2)$$

Although this expansion has been truncated to order 4, the code FOCEX can handle expansions to arbitrarily high orders provided there is enough computer memory to handle the higher-rank force constants. Besides this truncation in rank, the other approximation controlled by the user is in the truncation of the **range of interactions**. Furthermore, the FCs of the system are reduced based on permutation, translation, rotation and point or space group symmetries of the crystal. Hence, the FOCEX code first starts by identifying the symmetry properties and constructing the space group matrices S and translations, in order to define the set of irreducible or independent force constants, and their relationship to the full set of force constants.

2.1. Invariance under permutation of indices

From the above expression[2], it is evident that the FCs are derivatives of potential energy, so the order of derivatives does not matter and thus the indices of FCs can be arbitrarily swapped:

$$\Phi_{ij} = \Phi_{ji} \quad \Psi_{ijk} = \Psi_{ikj} = \Psi_{jik} = \Psi_{kji} = \dots \quad \chi_{ijkl} = \chi_{ikjl} = \chi_{ijlk} = \chi_{jilk} = \dots \quad (3)$$

2.2. Invariance under arbitrary translations and rotations

The potential energy of a solid remains the same under arbitrary translations and rotations of that solid. For any given atomic displacement u , the potential energy associated with the translation of the whole system by an arbitrary vector c is $V(u + c)$ and it must satisfy $V(u + c) = V(u)$ and $F(u + c) = F(u)$, where u are the dynamical variables and c is the arbitrary constant shift vector. Identifying terms order by order we arrive at the following equations Liebfried and Ludwig (1961):

$$\begin{aligned}
 0 &= \sum_{\tau} \Pi_{0\tau\alpha} \forall(\alpha) \quad (\text{Total force on unit cell} = 0) \\
 0 &= \sum_{R_1, \tau_1} \Phi_{0\tau, R_1 \tau_1}^{\alpha\beta} \forall(\alpha\beta, \tau) \\
 0 &= \sum_{R_2, \tau_2} \Psi_{0\tau, R_1 \tau_1, R_2 \tau_2}^{\alpha\beta\gamma} \forall(\alpha\beta\gamma, \tau, R_1 \tau_1) \\
 0 &= \sum_{R_3, \tau_3} \chi_{0\tau, R_1 \tau_1, R_2 \tau_2, R_3 \tau_3}^{\alpha\beta\gamma\delta} \forall(\alpha\beta\gamma\delta, \tau, R_1 \tau_1, R_2 \tau_2)
 \end{aligned} \tag{4}$$

These are the well-known *acoustic sum rules* generalized to higher-order FCs.

Similarly, the force on atoms and the total potential energy of the crystal should not change under arbitrary rotation of the crystal. This leads to the following constraints on FCs Liebfried and Ludwig (1961):

$$\begin{aligned}
 0 &= \sum_{\tau} \Pi_{0\tau\alpha} \tau^{\beta} \varepsilon^{\alpha\beta\nu}, \quad \forall(\nu) \quad (\text{Torque on unit cell} = 0) \\
 0 &= \sum_{R_1, \tau_1} \Phi_{0\tau, R_1 \tau_1}^{\alpha\beta} (R_1 + \tau_1)^{\gamma} \varepsilon^{\beta\gamma\nu} + \Pi_{0\tau}^{\beta} \varepsilon^{\beta\alpha\nu} \forall(\alpha\nu, \tau) \\
 0 &= \sum_{R_2, \tau_2} \Psi_{0\tau, R_1 \tau_1, R_2 \tau_2}^{\alpha\beta\gamma} (R_2 + \tau_2)^{\delta} \varepsilon^{\gamma\delta\nu} + \Phi_{0\tau, R_1 \tau_1}^{\gamma\beta} \varepsilon^{\gamma\alpha\nu} + \Phi_{0\tau, R_1 \tau_1}^{\alpha\gamma} \varepsilon^{\gamma\beta\nu} \forall(\alpha\beta\nu, \tau, R_1 \tau_1) \\
 0 &= \sum_{R_3, \tau_3} \chi_{0\tau, R_1 \tau_1, R_2 \tau_2, R_3 \tau_3}^{\alpha\beta\gamma\delta} (R_3 + \tau_3)^{\mu} \varepsilon^{\delta\mu\nu} + \Psi_{0\tau, R_1 \tau_1, R_2 \tau_2}^{\delta\beta\gamma} \varepsilon^{\delta\alpha\nu} + \Psi_{0\tau, R_1 \tau_1, R_2 \tau_2}^{\alpha\delta\gamma} \varepsilon^{\delta\beta\nu} \\
 &\quad + \Psi_{0\tau, R_1 \tau_1, R_2 \tau_2}^{\alpha\beta\delta} \varepsilon^{\delta\gamma\nu} \forall(\alpha\beta\gamma\nu, \tau, R_1 \tau_1, R_2 \tau_2)
 \end{aligned} \tag{5}$$

where $\varepsilon^{\alpha\beta\gamma}$ is the anti-symmetric Levi-Civita symbol. Moreover, an implicit summation over repeated cartesian indices is implied.

We see that rotational invariance relations relate the first to the second-order terms, the second to the third-order terms and the third to the fourth-order terms, respectively. This implies that if the expansion of the potential energy is truncated after the fourth order terms, we must start with the fourth order terms, and the application of the rotational invariance rules will give us constraints on the third and lower-order FCs. For more details on the proof regarding the translation and rotational invariance relations, we refer the reader to the article by Liebfried and Ludwig Liebfried and Ludwig (1961).

These invariances are usually not imposed in other methods, but become important in 2D materials to correctly describe the out-of-plane ZA modes and in 1D materials to describe the bending modes, both of which must have a quadratic dispersion at small phonon wavenumbers. For any simplified LD model to physically make sense, these invariances must be imposed.

In addition to these symmetries, it is important to note that elastic constants are subject to a number of constraints that enforces them to be symmetric under the exchange of Voigt indices. Huang discusses these invariances Born and Huang (1954), which provide an additional 15 set of constraint equations for low symmetry crystals with internal degrees of freedom in the primitive cell Sluiter, Weinert, and Kawazoe (1998, 1999)]. These relations are explicitly written in section 3 where we define the elastic constants.

2.3. Invariance under point or space group symmetry

Other symmetry operations such as rotations or mirror symmetries, elements of the space group also leave the potential energy of the crystal unaltered Maradudin and Fein (1962). In particular, force constants must be invariant under translations of lattice vectors, implying the following relations:

$$\begin{aligned}
 \Pi_{R\tau\alpha} &= \Pi_{0\tau\alpha} \forall(R\tau\alpha) \\
 \Phi_{R\tau, R_1 \tau_1}^{\alpha\beta} &= \Phi_{0\tau, (R_1 - R)\tau_1}^{\alpha\beta} \\
 \Psi_{R\tau, R_1 \tau_1, R_2 \tau_2}^{\alpha\beta\gamma} &= \Psi_{0\tau, (R_1 - R)\tau_1, (R_2 - R)\tau_2}^{\alpha\beta\gamma} \\
 \chi_{R\tau, R_1 \tau_1, R_2 \tau_2, R_3 \tau_3}^{\alpha\beta\gamma\delta} &= \chi_{0\tau, (R_1 - R)\tau_1, (R_2 - R)\tau_2, (R_3 - R)\tau_3}^{\alpha\beta\gamma\delta}
 \end{aligned} \tag{6}$$

These equations are used to restrict all the force constants to those whose first index is an atom in the central primitive cell ($R = 0$). This is how they are stored in the FOCEX code.

If the point or space group related operation S is governed by the matrix S then the following relations must hold:

$$\begin{aligned}
 \Pi_{S\tau\alpha} &= \sum_{\alpha'} \Pi_{\tau\alpha'} S_{\alpha,\alpha'} \\
 \Phi_{S\tau,S\tau_1}^{\alpha\beta} &= \sum_{\alpha'\beta'} \Phi_{\tau,\tau_1}^{\alpha'\beta'} S_{\alpha,\alpha'} S_{\beta,\beta'} \\
 \Psi_{S\tau,S\tau_1,S\tau_2}^{\alpha\beta\gamma} &= \sum_{\alpha'\beta'\gamma'} \Psi_{\tau,\tau_1\tau_2}^{\alpha'\beta'\gamma'} S_{\alpha,\alpha'} S_{\beta,\beta'} S_{\gamma,\gamma'} \\
 \chi_{S\tau,S\tau_1,S\tau_2,S\tau_3}^{\alpha\beta\gamma\delta} &= \sum_{\alpha'\beta'\gamma'\delta'} \chi_{\tau,\tau_1,\tau_2,\tau_3}^{\alpha'\beta'\gamma'\delta'} S_{\alpha,\alpha'} S_{\beta,\beta'} S_{\gamma,\gamma'} S_{\delta,\delta'}
 \end{aligned} \tag{7}$$

where $S_{\alpha,\alpha'}$ are the 3×3 matrix elements of the symmetry operation S , and $S\tau$ is the image of the atom τ under that space group transformation (including eventual glide operations in non-symmorphic groups).

All these symmetry relations impose a *linear* set of constraints on the force constants.

These invariance relations must be satisfied by any physically meaningful description of force constants. On the other hand, we approximate the Taylor expansion of the potential energy by truncating the range of FCs and their order. As a result, applying the constraints may slightly shift their value from its real numerical value, but it has the advantage that they are physical and, for instance, will replicate the linear acoustic phonon dispersion or quadratic out of plane in 2D or bending modes in 1D at $k = 0$. Therefore, one should be aware that an unrealistic truncation to a too small range may result in disagreement with experimental values. Therefore checks must be performed, and range increased until the results on phonon dispersions for instance do not change above some cut-off value.

2.4. Extraction procedure

To extract force constants of the LD model, we perform accurate calculations of forces on displaced atoms in a supercell, typically using DFT methods, and fit their values with the polynomial LD model described in Eq. (2). The set of invariance relations 4,5 and 7 form a (non-square) matrix relation of the form $[I]\Phi = 0$, while the force-displacement constraints is of the form $[U]\Phi = F$. These two parts are combined together, and a singular value decomposition (SVD) or rather a ridge regression algorithm is used to extract the independent FCs. The reason is that the above set of equations is usually an overcomplete set. Another option available to the user is to first fit (using SVD) true forces to Eq. (2), i.e. solve $[U]\Phi = F$ in a least squares sense, and then to project on the zero eigenvalue space of the $[I]$ matrix. This enforces the invariance relations (4), (5) and (7) more exactly, but at the cost of violating the $[U]\Phi = F$ relation.

It is to be noted that the data set obtained for force-displacement in fitting comes from a supercell. The size of supercell should exceed the range of FCs or else, the contribution of the images of atoms will also be included in the computed FCs: meaning for instance only the sum $\sum_L \Phi_{\tau,L+\tau'}^{\alpha\beta}$, where L is a supercell translation vector and τ and τ' are two atoms within the supercell, is accessible.

Additionally, FOCEX has the ability to read input force constants (typically harmonic) from a previous fit, and extract only the remaining non-fitted (typically cubic and quartic) FCs.

2.5. Phonon dispersion and their density of states

With the extracted force constants, and since the calculation does not take much time and resources, we have added to FOCEX the capability to calculate the phonon dispersion, density of states (DOS), mode Gruneisen parameters, the elastic tensor, and the thermodynamic properties within the quasi-harmonic approximation, which are all relatively fast calculations even on a laptop computer. We use the following definition for the $\alpha\beta$ components of dynamical matrix at the wavenumber k

$$D_{\tau,\tau'}^{\alpha\beta}(k) = \sum_R \frac{\Phi_{\tau,R+\tau'}^{\alpha\beta}}{\sqrt{m_\tau m_{\tau'}}} e^{ik \cdot (R+\tau'-\tau)} \tag{8}$$

This is a Hermitian matrix, the eigenvalues of which are the square of phonon frequencies at k , also satisfying completeness and orthonormality.

$$D_{\tau,\tau'}^{\alpha\beta}(k) e_{\tau'\beta,\lambda}(k) = \omega_\lambda^2(k) e_{\tau\alpha,\lambda}(k) \quad \text{and} \quad \sum_\lambda e_{\tau\alpha,\lambda}(k)^* e_{\tau'\beta,\lambda}(k) = \delta_{\alpha\beta} \delta_{\tau\tau'} \quad \text{and} \quad \sum_{\tau\alpha} e_{\tau\alpha,\lambda}(k)^* e_{\tau\alpha,\lambda}(k) = \delta_{\lambda\lambda'} \tag{9}$$

In other words, if one considers $\tau\alpha$ as the line index and λ as the column index of the eigenvector matrix, this matrix should be unitary. There is another choice for the phase of the dynamical matrix, which is to replace the factor $e^{ik.(R+\tau'-\tau)}$ in eq. 8 by $e^{ik.R}$. Both choices lead to the same phonon frequencies but the eigenvectors in the second case will be $e_{\tau\alpha,\lambda}(k)e^{-ik.\tau}$. However, the first choice leads to a continuous eigenvector as a function of k when the Brillouin zone is crossed. This choice of the definition of the dynamical matrix leads to well-defined group velocities, and that is what is implemented in FOCES. The expression for the group velocity is obtained by taking a wavevector derivative of the square of the phonon frequency ($\omega^2 = e.D.e \Rightarrow 2\omega v = e.(dD/dk).e$). Using the Hellmann-Feynman theorem applied to the derivative of the dynamical matrix, and dividing by $2\omega_\lambda(k)$ one finds:

$$v_\lambda^\gamma(k) = \frac{1}{2\omega_\lambda(k)} \sum_{\tau\alpha, R\tau'\alpha'} i(R + \tau' - \tau)^\gamma e_{\tau\alpha,\lambda}(k)^* \frac{\Phi_{\tau, R+\tau'}^{\alpha\beta}}{\sqrt{m_\tau m_{\tau'}}} e_{\tau\alpha,\lambda}(k) e^{ik.(R+\tau'-\tau)} \quad (10)$$

In case of degenerate bands, a rotation of the eigenvectors of the degenerate subspace will be needed to make dD/dk diagonal, leading to the correct group velocities on the diagonal.

The phonon density of states is calculated using both the tetrahedron method in the full first Brillouin zone (FBZ) and the Gaussian-smearing method in the irreducible Brillouin zone (IBZ). The latter will be inaccurate unless a large number of kpoints are used in the sampling of the IBZ, while the former is almost converged for a moderate grid size on the order of 20 k-mesh per direction.

2.6. Non-analytic correction for ionic dielectrics

For such systems, the input to the file `dielectric.params` which contains the electronic contribution to the dielectric matrix ϵ_∞ and the Born effective charges $Z_\tau^{\alpha\beta}$ of every atom τ in the primitive cell, must be properly initialized. These numbers are obtained from a separate DFPT calculation (Gonze and Lee (1997); Baroni, de Gironcoli, Dal Corso, and Giannozzi (2001)). The contribution of the ionic charges on the force constants is long-ranged and cannot be captured by the small supercell. It is usually calculated using the Ewald sum method (Ewald (1921); Ohno, Esfarjani, and Kawazoe (2018); Gonze and Lee (1997)), which is formed from the the sum of short-range real space component and a long-range reciprocal-space component. In FOCES, once the harmonic force constants are fitted, we calculate the dynamical matrix on a grid of reciprocal lattice vectors of the supercell inside the Wigner-Seitz cell of the primitive lattice, including its boundaries, albeit with a weight inversely proportional to the number of images that also fall on the Brillouin zone boundaries. This corresponds to the Fourier transform of the real-space force constants. Phonon frequencies on this grid, $D(G_{sc})$, are exact. From these dynamical matrices, we subtract the non-analytical contribution (Gonze and Lee (1997)), and Fourier transform back to real space, in-order to presumably obtain a short-ranged set of force constants, with a range confined to the Wigner-Seitz cell of the supercell. Then at an arbitrary wavevector q , we use Fourier interpolation to calculate the dynamical matrix from the latter set of force constants, to which the non-analytical part that was subtracted earlier, is added back (see also Togo, Chaput, Tadano, and Tanaka (2023)).

3. Some notes on Elastic constants

It is possible to extract the elastic constants from the knowledge of the force constants (Wallace (1998)). Below, we outline a simpler method and provide the final formulas.

Under a uniform applied strain, denoted by $\eta_{\alpha\beta} = \partial u_\alpha / \partial r_\beta$ a point x of the medium is moved to $x'_\alpha = x_\alpha + \eta_{\alpha\beta} x_\beta$, and the total energy of the harmonic crystal is increased, by definition of the elastic constants, by $\Delta E / V_0 = C_{\alpha\beta,\gamma\delta} \epsilon_{\alpha\beta} \epsilon_{\gamma\delta} / 2$, where V_0 is the unit cell volume and the Cauchy strain tensor ϵ is defined as $\epsilon_{\alpha\beta} = (\eta_{\alpha\beta} + \eta_{\beta\alpha}) / 2$. The latter is used because the antisymmetric part of the strain tensor η , represents a pure rotation and does not contribute to the total energy change. So, using the Cauchy strain, the 9 strains are reduced to 6 independent ones. Under such strain, we can use eq. 1 to calculate the potential energy increase by replacing u_i by:

$$u_{R\tau\alpha}(t) = \eta_{\alpha\beta} (R + \tau)^\beta + u_{\tau\alpha}^0 + y_{R\tau\alpha}(t) = S_{R\tau\alpha} + y_{R\tau\alpha}(t) \quad (11)$$

where S is the static displacement, containing an extra-term u^0 which represents the relaxation of atom τ within the primitive cell in addition to that due to the uniform deformation dictated by η . This can occur in low-symmetry crystals, where atoms may not completely follow the uniform deformation, and require an extra displacement $u_{\tau\alpha}^0$ to minimize

the potential energy. The last term $y_{R\tau\alpha}(t)$ represents the dynamical motion of the atom $R\tau$, or phonon degree of freedom, which has a time average of zero by construction. Plugging into eq. 1, we can derive the effective harmonic potential, at finite temperatures, as the coefficient of the y^2 term, and the elastic tensor as the second derivative of the average potential energy with respect to the applied (Cauchy) strain: $C_{\alpha\beta,\gamma\delta} = \frac{1}{V_0} \frac{\partial^2 E}{\partial \epsilon_{\alpha\beta} \partial \epsilon_{\gamma\delta}}$. Note that as a second derivative, C must be symmetric under swapping of the order of differentiation $\alpha\beta \longleftrightarrow \gamma\delta$. Due to the symmetry of the Cauchy strain tensor ϵ itself, the elastic tensor C will also be invariant with respect to swap of $\alpha \longleftrightarrow \beta$ and $\gamma \longleftrightarrow \delta$ separately.

Substitution of deformations S in eq. 1, keeping up to harmonic terms in S , leads to:

$$(V^{LD} - E_0)(S) = \sum_{R\tau\alpha} \Pi_{\tau\alpha} S_{R\tau\alpha} + \frac{1}{2} \sum_{R\tau\alpha, R'\tau'\alpha'} \Phi_{R\tau, R'\tau'}^{\alpha\alpha'} S_{R\tau\alpha} S_{R'\tau'\alpha'} + \dots \quad (12)$$

While this is valid strictly at zero temperature, this discussion can be extended to finite temperatures using the self-consistent phonon theory Werthamer (1970) where the harmonic force constant Φ is replaced by an effective temperature-dependent one Esfarjani and Liang (2020, 2022): $\Phi \rightarrow K(T) = \Phi + \Psi S + \chi(SS + \langle yy \rangle)/2$. In what follows, we will derive the (harmonic) elastic properties, strictly speaking, at zero temperature, but the above formula may be used as an extension to finite temperatures, by replacing every occurrence of Φ in the following by $K(T)$.

The stress σ is obtained by taking the first derivative of the energy in eq. 12 with respect to the Cauchy strain ϵ , while the second derivative gives the elastic tensor.

Compared to the method discussed by Wallace Wallace (1998), here, we are proposing an equivalent but simpler method to obtain elastic constants. We first write the harmonic potential energy in eq. 12, phenomenologically, up to second powers of internal coordinates u^0 and strain η as:

$$V^{LD}(\eta, u^0) = E_0 + \Pi_{\tau\alpha} u_{\tau\alpha}^0 + \Xi_{\mu\nu} \eta_{\mu\nu} + \frac{1}{2} \left[\phi_{\tau, \tau'}^{\alpha\alpha'} u_{\tau\alpha}^0 u_{\tau'\alpha'}^0 + A_{\alpha\beta, \alpha'\beta'} \eta_{\alpha\beta} \eta_{\alpha'\beta'} + 2Q_{\tau\alpha, \alpha'\beta'} u_{\tau\alpha}^0 \eta_{\alpha'\beta'} \right] \quad (13)$$

As before, sums over repeated indices are implied. By comparing this equation with eq. 1 in which $u_{R\tau\alpha}$ is replaced by $\eta_{\alpha\beta}(R + \tau)^\beta + u_{\tau\alpha}^0$, the new coefficients A, Q, ϕ can be identified with the harmonic force constants Φ through the following relations:

$$\Xi_{\alpha\beta} = \frac{1}{N} \sum_{R\tau} \Pi_{\tau\alpha} (R + \tau)^\beta = \sum_{\tau} \Pi_{\tau\alpha} \tau^\beta \quad (14)$$

$$\phi_{\tau, \tau'}^{\alpha\alpha'} = \frac{1}{N} \sum_{R, R'} \Phi_{R\tau, R'\tau'}^{\alpha\alpha'} \quad \text{with} \quad \phi_{\tau, \tau'}^{\alpha\alpha'} = \phi_{\tau', \tau}^{\alpha'\alpha}; \quad \text{ASR} \Rightarrow \sum_{\tau} \phi_{\tau, \tau'}^{\alpha\alpha'} = \sum_{\tau'} \phi_{\tau, \tau'}^{\alpha\alpha'} = 0 \quad (15)$$

$$Q_{\tau\alpha, \alpha'\beta'} = \frac{1}{N} \sum_{RR'\tau'} \Phi_{R\tau, R'\tau'}^{\alpha\alpha'} (R' + \tau')^{\beta'} = \frac{1}{N} \sum_{RR'\tau'} \Phi_{R\tau, R'\tau'}^{\alpha\alpha'} (R' + \tau' - R - \tau)^{\beta'} \quad \text{ASR} \Rightarrow \sum_{\tau} Q_{\tau\alpha, \alpha'\beta'} = 0 \quad (16)$$

$$A_{\alpha\beta, \alpha'\beta'} = \frac{1}{N} \sum_{R\tau, R'\tau'} \Phi_{R\tau, R'\tau'}^{\alpha\alpha'} (R + \tau)^\beta (R' + \tau')^{\beta'} \quad \text{with} \quad A_{\alpha\beta, \alpha'\beta'} = A_{\alpha'\beta', \alpha\beta} \quad (17)$$

In addition to translational invariance (ASR), rotational invariance implies $Q_{\tau\alpha, \beta\gamma} \epsilon^{\alpha\beta\gamma} = 0; \forall \tau$. Even though, due to translational symmetry of the crystal, the above sums do not depend on the vectors R , we have kept them in the summation for the sake of symmetry in the formulas, but divided by N , the (infinite) number of translation vectors R . If there are N_0 sites in the primitive cell, Π is a $3N_0$ component array, ϕ and Q are respectively a $3N_0 \times 3N_0$ and $3N_0 \times 6$ matrices, while A is will be a 6×6 matrix if the Voigt notation is used to describe the strain and stress tensors. Voigt notation is used after symmetrizing A and Q since the potential energy should not depend on the rotational part of the strain η .

The key point in calculating the elastic tensor, which is the second strain-derivative of V^{LD} , is to first relax the crystal by minimizing the potential energy with respect to u^0 . This corresponds to the equilibrium condition: $\frac{\partial V^{LD}}{\partial u_{\tau\alpha}^0} = 0 = \Pi + \phi u^0 + Q\eta \Rightarrow u^0(\eta) = -\Gamma(\Pi + Q\eta)$ where the matrix Γ is the inverse of ϕ : $\sum_{\tau', \alpha'} \Gamma_{\tau, \tau'}^{\alpha\alpha'} \phi_{\tau', \tau}^{\alpha'\alpha''} = \delta_{\alpha\alpha''} \delta_{\tau\tau''}$.

Note that since ϕ has three acoustic modes of zero eigenvalue, it is not invertible. Fixing the residual displacement of atom 1 to be $u_1^0 = 0$ makes ϕ an invertible $(3N_0 - 3) \times (3N_0 - 3)$ matrix, so that in the sums over primitive cell atoms τ one should exclude the first atom, or alternatively, one can pad the matrix Γ by 0 to make it $3N_0 \times 3N_0$.

$$u_{\tau\alpha}^0(\eta) = -\Gamma_{\tau, \tau'}^{\alpha\alpha'} (\Pi_{\tau'\alpha'} + Q_{\tau'\alpha', \mu\nu} \eta_{\mu\nu}); \quad \text{with} \quad \Gamma_{1, \tau'}^{\alpha\alpha'} = \Gamma_{\tau, 1}^{\alpha\alpha'} = 0 \quad \text{leading automatically to} \quad u_{1\alpha}^0 = 0. \quad (18)$$

Note that even in the absence of strain ($\eta = 0$), if there is a residual force $\Pi_{\tau\alpha}$ in the reference configuration, equation 18 predicts the atom τ should relax to its equilibrium position given by: $u_{\tau\alpha}^0 = -\Gamma_{\tau,\tau'}^{\alpha\alpha'} \Pi_{\tau'\alpha'}$.

After relaxing the internal coordinates u^0 , and substituting the formula in eq. 18 for u^0 in eq. 13, the potential energy becomes a function of strain η only:

$$V_{relaxed}^{LD}(\eta) = E_0 - \frac{1}{2} \Pi_{\tau\alpha} \Gamma_{\tau\alpha,\tau'\alpha'} \Pi_{\tau'\alpha'} + \Xi_{\mu\nu} \eta_{\mu\nu} - \Pi_{\tau\alpha} \Gamma_{\tau\alpha,\tau'\alpha'} Q_{\tau'\alpha';\mu\nu} \eta_{\mu\nu} + \frac{1}{2} (A_{\mu\nu,\mu'\nu'} - Q_{\tau\alpha;\mu\nu} \Gamma_{\tau\alpha,\tau'\alpha'} Q_{\tau'\alpha';\mu'\nu'}) \eta_{\mu\nu} \eta_{\mu'\nu'} \quad (19)$$

Finally, the first and second strain derivatives give respectively the residual stress and the elastic tensor. Using the chain rule to convert η derivatives to ϵ derivatives, essentially boils down to symmetrizing the results (in effect, the symmetric parts of A or Q come in the results as previously mentioned).

$$\sigma_{residual} = \frac{dV_{relaxed}^{LD}}{V_0 d\eta} = \frac{dV_{relaxed}^{LD}}{V_0 d\epsilon} = \frac{1}{V_0} \text{Symmetrized}(\Xi - \Pi \Gamma Q) \quad (20)$$

$$C = \frac{1}{V_0} \frac{d^2}{d\epsilon^2} V_{relaxed}^{LD}(\epsilon, u_{relaxed}^0(\epsilon)) = \frac{1}{V_0} \text{Symmetrized}(A - Q \Gamma Q) \quad (21)$$

where V_0 is the equilibrium unit cell volume, and $\text{Symmetrized}(B_{\mu\nu}) = \frac{1}{2}(B_{\mu\nu} + B_{\nu\mu})$ and $\text{Symmetrized}(B_{\mu\nu,\mu'\nu'}) = \frac{1}{4}(B_{\mu\nu,\mu'\nu'} + B_{\nu\mu,\mu'\nu'} + B_{\mu\nu,\nu'\mu'} + B_{\nu\mu,\nu'\mu'})$. While in the elastic tensor, the first term A is the second *partial* derivative of the potential energy with respect to strain, the second term $Q \Gamma Q$ is the correction due to the atomic relaxations u^0 , reflecting that the elastic constant is the full second derivative. Note that due to the symmetry of ϕ and thus of Γ , this term is also symmetric with respect to interchange of $\mu\nu \leftrightarrow \mu'\nu'$.

Similar to eq. 18, which gives the *relaxed positions* of the primitive cell atoms in the reference configuration, one can also, get the final *relaxed shape* of the primitive cell in terms of the residual stress in eq. 20:

$$\frac{dV_{relaxed}^{LD}}{V_0 d\epsilon} = 0 = \sigma_{residual} + C\epsilon \Rightarrow \epsilon^{eq} = -C^{-1} \sigma_{residual} \quad (22)$$

Note that even if the reference configuration is not exactly the total energy minimum, due to incomplete or unconverged numerical relaxation, eqs. 22 and 18 can in principle be applied (in this order as eq. 18 involves the strain) to further relax the reference primitive cell (these corrections are non-zero only if $\Pi \neq 0$). This can happen in crystals of low symmetry, where space group symmetry constraints do not imply $\Pi = 0$. In cases where $\Pi = 0$ due to symmetry, such as in Ge, there might additionally be a residual stress because the lattice constant relaxation was not complete. This residual stress is however available at the end of the DFT-SCF relaxation and should be added to the expression for $\sigma_{residual}$ if the equilibrium strain in eq. 22 is needed.

Also note that since typically force constants are on the order of 10 eV/\AA^2 , if the residual force is on the order of $\Pi \simeq 10 \text{ meV/\AA}$, the corresponding required atomic relaxation would be on the order of $u_{\tau}^0 \simeq \Pi_{\tau} / \phi_{\tau,\tau} \simeq 0.001 \text{ \AA}$ and therefore usually small.

The isotropic and uniaxial elastic constants are denoted respectively by the Bulk and Young moduli B and Y .

3.1. Bulk modulus

The isothermal bulk modulus is defined as $B_T = -V \left(\frac{dP}{dV} \right)_{P=0,T}$. The isotropic compression condition translates into $\sigma_{xx} = \sigma_{yy} = \sigma_{zz} = -P$; $\sigma_{\alpha\beta} = 0$ for $\alpha \neq \beta$, and since the volume change is given by $\Delta V/V = \epsilon_{xx} + \epsilon_{yy} + \epsilon_{zz} = \text{Tr } \epsilon$, one can express B in terms of elastic or compliance tensor elements as:

$$B = \frac{\text{Tr } \sigma / 3}{\text{Tr } \epsilon} = \frac{1}{9} \sum_{i,j=1,2,3} C_{ij} = \frac{1}{\sum_{i,j=1,2,3} S_{ij}} \quad (23)$$

where S is the inverse of C when written as a 6×6 matrix in the Voigt notation, and is called the *compliance tensor*. For crystals of cubic symmetry, it can be simplified as: $(C_{11} + 2C_{12})/3$.

3.2. Shear modulus

The shear stress μ_{xy} is the ratio $\left(\frac{\partial\sigma_4}{\partial\epsilon_4}\right)_{\sigma_{j\neq 4}=0}$. It can therefore be written as: $\mu = 1/S_{44}$. In some works, however, in order to average over anisotropy, e.g. when dealing with polycrystalline samples, where the elastic properties are supposed to be isotropic, usually the formula $\mu_{iso} = (C_{11} - C_{12} + 3C_{44})/5$, and more generally $\mu_{iso} = (C_{ii} - C_{jj} + 3C_{ll})/15$ where $i, j = 1, 2, 3; l = 4, 5, 6$, is reported for μ . To agree with the convention used in Materials Project, we also report this value for Ge in table 1.

3.3. Young modulus

The Young modulus along x is the response to a uniaxial deformation in that direction: $Y = \left(\frac{d\sigma_1}{d\epsilon_1}\right)_{\sigma_{j>1}=0} = \frac{1}{S_{11}}$.

But for isotropic materials, usually $Y_{iso} = 9\mu_{iso}B/(3B + \mu_{iso})$, where B and μ are defined above, is reported.

3.4. Poisson ratio

Finally, for a uniaxial deformation along the x axis, the Poisson ratio is defined as $\nu = -\left(\frac{\partial\epsilon_2}{\partial\epsilon_1}\right)_{\sigma_{i\neq 1}=0} = -\frac{S_{21}}{S_{11}}$.

Again, for isotropic materials, usually the value $\nu_{iso} = (1.5B - \mu_{iso})/(3B + \mu_{iso})$ is reported.

As noted, the values of Y , μ and ν would depend on the direction of applied stress with respect to crystalline axes in the case of anisotropic materials, where more care needs to be taken when investigating elastic properties theoretically or experimentally.

3.5. Mode Gruneisen parameters

The mode Gruneisen parameters are obtained from the phonons and the cubic force constants. They represent the change in the phonon frequencies under applied strain. Even though the strain is usually considered to be isotropic compression or dilation, one can also define the response to an arbitrary strain. By definition, we have $\gamma_{\lambda,\mu\nu} = -\frac{d\ln\omega_\lambda}{3d\epsilon_{\mu\nu}}$.

But usually the volume derivative, which corresponds to an isotropic strain is considered: $\gamma_\lambda = -\frac{d\ln\omega_\lambda}{d\ln V}$ where V is the unit cell volume. Applying a uniform hydrostatic strain $\epsilon_{\alpha\beta} = \delta_{\alpha\beta} dV/3V = \delta_{\alpha\beta} d\ln V/3$. Similar to the group velocity, we start with the square of the frequency written as the product of the dynamical matrix by eigenvectors: $\omega^2 = e.D.e$ and consider the change in D under strain: $dD/d\eta = \sum_R d\Phi/d\eta e^{ik.R}$, and use $d\Phi/d\eta = \Psi(R + \tau + du^0/d\eta)$. Note the latter term, which is non-zero for low-symmetry structures having their own internal relaxation under strain $u^0(\eta)$, is often neglected in the literature. In the previous section, we derived this equation $u^0(\eta) = -\Gamma(\Pi + Q\eta)$ for u^0 in the harmonic approximation. Therefore $du^0/d\eta = -\Gamma Q$. Using the Hellmann-Feynman theorem applied to the derivative of the dynamical matrix, and substituting the above relation for the strain derivative of the harmonic force constants, we finally find:

$$\gamma_\lambda(k) = -\frac{1}{6\omega_\lambda^2(k)} \sum_{\tau, R_1\tau_1, R_2\tau_2} \frac{\Psi^{\alpha\alpha_1\alpha_2}_{\tau, R_1\tau_1, R_2\tau_2}}{\sqrt{m_\tau m_{\tau_1}}} e_{\tau\alpha, \lambda}(k)^* e_{\tau_1\alpha_1, \lambda}(k) e^{ik.(R_1+\tau_1-\tau)} \left[(R_2 + \tau_2)^{\alpha_2} - \sum_{\mu=1,2,3} \Gamma_{\tau_2\alpha_2} \cdot Q_{\dots\mu\mu} \right] \quad (24)$$

The temperature-dependent Gruneisen parameter is defined to be the thermal average of the above modes weighted by their heat capacity: $\gamma(T) = \sum_{k\lambda} c_{k\lambda}(T)\gamma_\lambda(k) / \sum_{k\lambda} c_{k\lambda}(T)$, where the heat capacity per mode is $c_{k\lambda}(T) = k_B x_{k\lambda}^2 / \sinh^2 x_{k\lambda}$ and $x_{k\lambda} = \hbar\omega_\lambda(k)/2k_B T$.

3.6. Thermodynamic properties within the quasi-harmonic approximation (QHA)

The simplest way to calculate thermodynamic properties at finite temperatures is to use the QHA, which consists of assuming the T -dependence comes only through a volume dependence caused by thermal expansion. A given property \mathcal{P} needs only to be calculated as a function of volume, and once the relationship $V(T)$ or the thermal expansion is known, the temperature can be associated to the corresponding volume and the properties calculated as: $\mathcal{P}^{QHA}(T) \approx \mathcal{P}(V(T))$. To avoid calculation of force constants and phonons at different volumes, we use the definition of the Gruneisen parameter as given in eq.24 to obtain phonon frequencies at different volumes. Then the harmonic free energy at a given temperature T is the sum of electronic and vibrational contributions, and calculated using the following formula, which is the sum of zero temperature energy as a function of volume and the vibrational harmonic part:

$$F^{QHA}(T) \approx F(V(T)) = E_0(V(T)) + k_B T \sum_\lambda \ln [2 \sinh(\hbar\omega(V(T))/2k_B T)] \quad (25)$$

Here we are neglecting the electronic contribution to the free energy which may become important for metals, and is usually negligible for larger gap materials. At a fixed temperature T , this function can be minimized with respect to the volume to yield the equilibrium volume $V(T)$ to be used in eq. 25.

For the zero-temperature part of the free or total energy E_0 one can either assume $E_0(V) = E_0(V_0) + \frac{1}{2V_0} B(V - V_0)^2$, with B being the bulk modulus, or just use the Taylor expansion 19 in powers of η and replace volume derivatives by strain derivatives: $d \ln V = dV/V_0 = 3d\epsilon$, so that the zero-temperature equation of state can be written as:

$$E_0(V) = E_0(V_0) + \frac{(V - V_0)}{3V_0} \frac{dE_0}{d\epsilon} + \frac{(V - V_0)^2}{18V_0^2} \frac{d^2E_0}{d\epsilon^2} + \frac{(V - V_0)^3}{162V_0^3} \frac{d^3E_0}{d\epsilon^3} + \dots \quad (26)$$

where the strain derivatives are:

$$\frac{dE_0}{d\epsilon} = \text{Tr}_\alpha \left[\Xi_{\alpha\alpha} - \sum_{\tau\tau'\alpha'} \Pi_{\tau\alpha} \Gamma_{\tau\alpha;\tau'\alpha'} Q_{\tau'\alpha';\alpha\alpha} \right]; \quad \frac{d^2E_0}{d\epsilon^2} = V_0 \sum_{ij=1,2,3} C_{ij} \quad (27)$$

The third derivative can be easily obtained only if $u^0 = 0$ due to symmetry; otherwise the expression becomes complicated, due to the fact that equation 13 has to be extended to third-order and equation 18 would not be linear in η anymore, and needs to be solved for η and η be substituted back into 13 before taking the derivatives. Only in the case where $u^0 = 0$ or $du^0/d\eta = 0$, do we have

$$\frac{d^3E_0}{d\epsilon^3} (u^0 = 0; du^0/d\eta = 0) = \frac{1}{6N} \sum_{R_i\tau_i\alpha_i} \Psi_{R_1\tau_1,R_2\tau_2,R_3\tau_3}^{\alpha_1\alpha_2\alpha_3} (R_1 + \tau_1)^{\alpha_1} (R_2 + \tau_2)^{\alpha_2} (R_3 + \tau_3)^{\alpha_3}$$

In this case, we can also deduce the dimensionless parameter, so-called $B'_0 = dB/dP = (V_0 d^3E/dV^3)/(d^2E/dV^2)$.

To find the volume dependence of the phonon frequencies, we use $d\omega_\lambda/dV = -\gamma_\lambda\omega_\lambda/V$, and can finally find the equilibrium volume $V_{eq}(T)$ by minimizing F^{QHA} with respect to the strain or the volume.

Since the bulk modulus itself is a function of T , or, within the QHA, of the volume, we need to consider this dependence in the first term of the free energy when performing volume-minimization. The simplest volume dependence of the bulk modulus is a linear one. So we take $B(V) = B(V_0)(1 - B'_0(V - V_0)/V_0)$. In FOCEX, to include a temperature-dependence in the bulk modulus, we therefore use $B(V) = B(V_0)(1 - 3\eta_{eq}(T)B'_0)$. Note that only for materials with no internal relaxations u^0 can we calculate and use B'_0 .

3.7. Optical properties

The static dielectric constant is the sum of the ion-clamped (electronic) dielectric constant ϵ_∞ coming from a DFPT calculation, and the dielectric ionic polarizability: $\epsilon_0^{\alpha\beta}(\omega) = \epsilon_\infty^{\alpha\beta} + \chi^{\alpha\beta}(\omega)$ where:

$$\chi^{\alpha\beta}(\omega) = \frac{1}{4\pi\epsilon_0} \frac{4\pi e^2}{V_0} \sum_{\lambda>4} \frac{z_\lambda^{\alpha*} z_\lambda^\beta}{-\omega^2 + \omega_\lambda^2 - i\eta^2} \quad (28)$$

where η is a smearing factor reflecting anharmonicity or disorder, typically on the order of inverse phonon lifetimes, and $z_\lambda^\alpha = \sum_\tau Z_\tau^{\alpha\beta} e^{\tau\beta} (k=0)/\sqrt{m_\tau}$ is the dipole moment induced by the optical mode λ at the zone center ($k=0$). Its square $\sum_\alpha |z_\lambda^\alpha|^2$ is proportional to the IR peak intensity. This optical ionic response is in the IR domain where the excitation frequency is on the order of phonon vibrational frequencies.

3.8. Brief algorithm

1) There are 5 small input files which need to be prepared first: `default.params`, `structure.params`, `dielectric.params`, `latdyn.params`, `kpbs.params`.

2) Force-displacement supercell data must be stored in files named `POSCAR1`, `POSCAR2`, ... ; `FORCEDISP1`, `FORCEDISP2`, ... The FOCEX code checks consistency between the atomic structures of the supercell and the primitive cell described in `structure.params`. Force data may come from supercells of different shapes. Data for each shape is stored in a different input `POSCARi`, ... ; `FORCEDISPi`, ... $i=1,2,\dots$. Typically one large supercell

can be used to extract the harmonic FCs, which can be of long range, and a smaller supercell can be used for large-amplitude anharmonic displacements. The files POSCAR*i* contain the equilibrium or reference coordinates of the atoms in the supercell number *i*, in the POSCAR format defined in VASP.

3) Space group symmetries of the crystal are identified from the primitive cell information provided in `structure.params`.

4) The mapping between selected (according to their range) independent FCs and the full set of FCs for each rank is established according to Eqs.(3) to Eqs.(7).

5) The invariance relations, based optionally on translations (Eqs.(4), rotations (Eqs. (5)) and Huang constraints are coded in a matrix we label by $[I]$. These are a set of linear relations on unknown FCs which will be the homogeneous part of the linear matrix $[A]$ equation to solve.

6) Based on displacements in the supercell(s), the second block of the $[A]$ matrix, as well as the inhomogeneous part of the array b containing the forces are setup according to Eqs. (2). So the first block of matrix $[A]$ contains coefficients reflecting invariances and the second block contains first or higher powers of displacements.

7) The linear, over-determined system $A\Phi = b$ is solved using a singular-value decomposition (SVD) or ridge regression algorithm. The unknown array Φ contains the selected independent force constants.

8) Results are written into several files that can be used for testing and further analysis.

9) Finally, using the harmonic FCs, the phonon dispersion, density of states (dos), Gruneisen parameters, elastic constants and some thermodynamic properties based on QHA and dielectric constant are calculated and written into files.

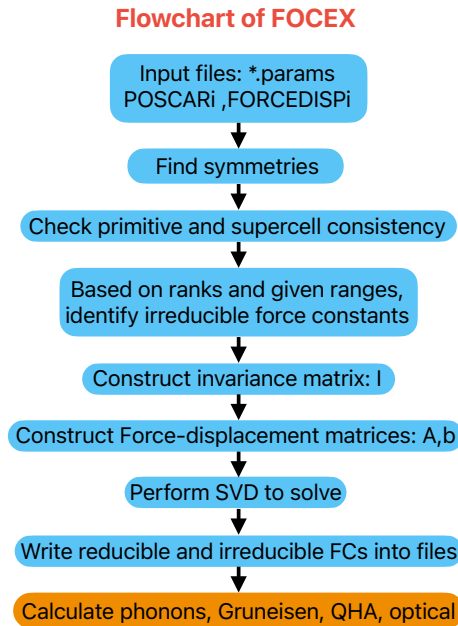


Figure 1: Workflow of FOCEX

3.9. Input files

The following files need to be present in the folder where the code FOCEX is run:

0) `default.params` file contains some of the less-used parameters which can be initialized if their default values do not work. This file needs to be present with lines initialized by 0 (in case the default has to be used), otherwise the defaults can be overwritten by whatever number appears on that line. The first line is the tolerance to equate two

coordinates (it is 0.002 Ang), the second is the regularization parameter in the ridge regression and is set to 1E-10. The third is the number of translation vectors defining the outer shell of neighbors. It is set to 7, and can be increased if the supercell is larger than 12 translation vectors. The user does not need to touch this file, but it needs to be present in the working directory.

1) The unit cell information and type and range of force constants to be fitted are specified in the file `structure.params`. These include conventional and primitive lattice vectors, atom identities: (name, mass, and positions in reduced units of the conventional cell), number of neighbors to include for each rank, options for symmetries to impose (translational, rotational and Huang), options for rank of force constants (2,3,4, ... up to 8) to be included in the fitting.

2) The dielectric matrix ϵ_∞ and Born charges Z_τ , in the same order as they appear in the `structure.params` file are read from the `dielectric.params` file. The dielectric matrix and Born charges are obtained from a separate DFPT calculation.

3) The information regarding the reference supercells are read from files `POSCAR1`, `POSCAR2`, ... written in the same format as VASP `POSCAR` file. The corresponding cartesian displacements (in Ang) and forces (in eV/Ang) are read from files `FORCEDISP1`, `FORCEDISP2`, ... Each `FORCEDISPi` file contains all the force-displacement snapshots corresponding to the i^{th} supercell defined in `POSCARi`. Each snapshot is separated from the next one by two lines, the first of which should contain the word "POSITION" and the second one contains the total energy of that snapshot. The N following lines contain the cartesian coordinates of the N atoms followed by the forces acting on them (6 columns in total).

4) The file `kpbs.params` contains the list of kpoints to use for the phonon band structure calculations. After the force constants are extracted, the `FOCEX` code also computes the harmonic properties, namely the phonon band structure, elastic and thermodynamic properties.

5) The input file `latdyn.params` contains information needed for the thermodynamic properties, namely the size of the k-point mesh in the first-Brillouin zone, the frequency mesh for the density of states, the smearing factor, and finally the temperature window for the thermodynamic properties.

3.10. Output files

Many output files are generated after the run. Many of them are used to test the validity of the output in case something goes wrong. The main useful files are:

1) `fc1_irr.dat`, `fc2_irr.dat`, `fc3_irr.dat`, `fc4_irr.dat`, ... contain the irreducible FCs (selected based on crystal symmetries and imposed range).

2) `fc1.dat`, `fc2.dat`, `fc3.dat`, `fc4.dat`, ... contain the full set of FCs, in separate files for ranks 1, 2, 3, 4 ... Each line contains the atom labels $R_i\tau_i$ involved, the cartesian coordinates α_i and the FC value $\frac{\partial^n V}{\partial u_{R_1\tau_1\alpha_1} \partial u_{R_2\tau_2\alpha_2} \dots}$.

3) `lat_fc.dat` contains the information on the primitive cell and neighboring cells, as well as the number of independent and dependent force constants.

4) `log-<extra>.dat` contains the log of the run, where the parameters "<extra>" label the type of the run, as described in the file `ios.f90`.

5) `mech.dat` contains the mechanical properties (elastic constants, etc...).

6) `thermo_QHA.dat` contains the thermodynamic properties: temperature, total energy, free energy, heat capacities, entropy, equilibrium QHA-volume, thermal expansion coefficient and average Gruneisen parameter.

7) `temp_free.dat` contains the free energy, pressure, Gruneisen parameter and bulk modulus in the (V, T) plane.

8) `bs_grun.dat` and `bs_freq.dat` both contain the band structure. While the first also has the gruneisen parameters, the second contains phonon group velocities. The same data in the irreducible Brillouin zone is written in `ibz_bands.dat` with group velocities, `ibz_grun.dat` with Gruneisen parameters.

9) `ibz_dos.dat` contains the Gaussian-smearred DOS from kpoints generated in the IBZ, while `fbz_dos.dat` contains the DOS generated using the tetrahedron method.

10) `chi_real.dat` and `chi_imag.dat` contain the 9 matrix elements of the real and imaginary parts of the ionic polarizability versus frequency.

11) Other auxiliary files contain information on the matrix $[A]$ (`amatrx.dat`) and the data generated during the SVD procedure (`svd-results.dat`), and many other files used for book-keeping and debugging, not necessarily of use to the user.

3.11. Utilities

Some utilities (`read_outcar.f90` and `read_qe.f90`) are also provided to convert the log or output files from a single snapshot of VASP (OUTCAR) or Quantum Espresso to FORCEDISP format. A shell script `xtract.sh` then calls these executables, and appends the output from each snapshot into the file `FORCEDISP1`. In addition, files for plotting the outputs using the Gnuplot software are also provided. `all.plt` or `bvel.plt` plot the phonon band structure, Gruneisen parameters DOS, and the group velocities. `KTICS.BS` should be imported in this file. `fcs.plt` plots the harmonic force constants versus pair distance and visualizes them in the Wigner-Seitz cell associated with the supercell. `qha.plt` plots the results from the QHA calculations: total energy, free energy, strain, volume, heat capacity, entropy and bulk modulus versus temperature. `kp.plt` visualizes the full zone, irreducible zone and band structure kpoints in 3d reciprocal space.

4. ANFOMOD

The code **ANFOMOD** performs molecular dynamics simulations with the anharmonic force field developed by FOCEX. It takes as input the output files of FOCEX: `lat_fc.dat`, `fc1.dat`, `fc2.dat`, `fc3.dat`, `fc4.dat`. It also has its own control file `anh_md.params` in which the type of run (NVE or NVT), duration, timestep, temperature, are specified. Finally, supercell information and cartesian atomic coordinates are read from `coordinates.sc` in VASP POSCAR format.

Using the polynomial force field, assuming the residual force $-\Pi$ is zero, the force acting on an atom $R\tau$ is given by:

$$F_{R\tau}^{\alpha LD} = - \sum_{R_1\tau_1} \Phi_{R\tau,R_1\tau_1}^{\alpha\beta} u_{R_1\tau_1}^{\beta} - \sum_{R_1\tau_1,R_2\tau_2} \frac{1}{2} \Psi_{R\tau,R_1\tau_1,R_2\tau_2}^{\alpha\beta\gamma} u_{R_1\tau_1}^{\beta} u_{R_2\tau_2}^{\gamma} - \sum_{R_1\tau_1,R_2\tau_2,R_3\tau_3} \frac{1}{6} \chi_{R\tau,R_1\tau_1,R_2\tau_2,R_3\tau_3}^{\alpha\beta\gamma\delta} u_{R_1\tau_1}^{\beta} u_{R_2\tau_2}^{\gamma} u_{R_3\tau_3}^{\delta} \quad (29)$$

To insure translational invariance, in the actual code the quantity $u_{R\tau}$ has been subtracted from every single displacement, i.e. $u_{R_1\tau_1}^{\beta}$ is replaced by $u_{R_1\tau_1}^{\beta} - u_{R\tau}^{\beta}$, and so on.

To update atomic positions, the standard velocity Verlet Ohno et al. (2018) algorithm is used. If canonical ensemble needs to be simulated, a Langevin thermostat, in which the damping rate can be adjusted, has been adopted. A good initial guess for the latter would be $1/(1000dt)$ where dt is the MD timestep.

The heat current is formulated from the following definition: $J^{\alpha} = \sum_{R\tau} j_{R\tau}^{\alpha}$ where R runs over the primitive cells in the simulation supercell, and where the local heat current is defined as:

$$j_{R\tau}^{\alpha} = \frac{1}{4} \sum_{R_1\tau_1} (R_1 + \tau_1 - R - \tau)^{\alpha} f_{R\tau,R_1\tau_1}^{\beta} (v_{R_1\tau_1} + v_{R\tau})^{\beta} \quad (30)$$

where $f_{R\tau,R_1\tau_1}^{\beta} = \frac{\partial \mathcal{V}_{R\tau}}{\partial u_{R_1\tau_1}^{\beta}}$ is the effective pair force between $R\tau$ and $R_1\tau_1$. $\mathcal{V}_{R\tau}$ is the local potential energy of site $R\tau$:

$$\mathcal{V}_{R\tau} = \sum_{\alpha} u_{R\tau}^{\alpha} \left[\sum_{R_1\tau_1} \frac{1}{2} \Phi_{R\tau,R_1\tau_1}^{\alpha\beta} u_{R_1\tau_1}^{\beta} + \sum_{R_1\tau_1,R_2\tau_2} \frac{1}{3!} \Psi_{R\tau,R_1\tau_1,R_2\tau_2}^{\alpha\beta\gamma} u_{R_1\tau_1}^{\beta} u_{R_2\tau_2}^{\gamma} + \sum_{R_1\tau_1,R_2\tau_2,R_3\tau_3} \frac{1}{4!} \chi_{R\tau,R_1\tau_1,R_2\tau_2,R_3\tau_3}^{\alpha\beta\gamma\delta} u_{R_1\tau_1}^{\beta} u_{R_2\tau_2}^{\gamma} u_{R_3\tau_3}^{\delta} \right] \quad (31)$$

The total, kinetic and potential energy as well as the heat current will be written in separate files at a given output-rate. To obtain the thermal conductivity using the Green-Kubo formula, the heat current data needs to be post-processed.

5. Other codes

Other codes have been developed which will read the FOCEX outputs, namely `fci.dat` ($i=2,3,4,\dots$) and `lat_fc.dat` to compute other physical properties. Details about these codes will be published elsewhere.

- **THERMACOND** computes the thermal conductivity as the solution to the Boltzmann transport equation within and beyond the relaxation time approximation (RTA).
- **SCOP8** calculates for a given temperature, the state of equilibrium of the crystal, namely its primitive cell shape and size as well as the atomic coordinates, and the renormalized force constants calculated within the self-consistent phonon (SCP) approximation.

6. Installation

The ALADYN software package is available on GitHub under GPL-3.0 license at <https://github.com/KeivanS/Anharmonic-lattice-dynamics>, where each code is stored in the corresponding subdirectory. A `Makefile` template for each code has been provided. After cloning the repository, the user can type `make` to generate all needed executables, or alternatively go into each subdirectory, edit the `Makefile` according to their system and needs, and run `make`. The codes can be compiled using the GNU Fortran Compiler `gfortran` or the Intel Fortran Compiler `ifort`, and are tested to be compatible with `gfortran` versions 7-11 and `ifort` versions 18-19. (Newer and/or older versions are likely to be compatible as well.) The only external library is the `zhegv` diagonalization routine from LAPACK. A successful compilation results in the creation of the `ALADYN_BIN` directory containing all the executables.

In a typical high-performance computing cluster environment, one should be able to compile the codes using commands similar to the following. For example, to compile FOCEX with GCC (assuming `gfortran` is the installed fortran compiler):

```
module load gcc
git clone https://github.com/KeivanS/Anharmonic-lattice-dynamics
cd Anharmonic-lattice-dynamics/FOCEX
make
```

assuming GCC is preinstalled as a module on the cluster.

7. Example of Ge, and some tips

Here we show the example of Germanium as a system ran with FOCEX. We must emphasize that the force-displacements inputs stored in `FORCEDISP1` are up to the user. For a choice of the supercell and magnitude of displacements, the best set of FCs will be extracted. But the results will change with a change in the supercell, magnitude of displacements, choice of the exchange-correlation potential, lattice parameter, chosen rank and chosen range of FCs. So it is up to the user to make sure the obtained results are converged. As a rule of thumb, a supercell of 100 atoms or more is usually enough to provide a very reasonable set of force constants. To get accurate harmonic force constants, displacements need to be small enough. Typically displacements on the order of or less than 0.05 \AA are reasonable. While many codes require moving one or two atoms at the most, in FOCEX all atoms maybe simultaneously moved, providing more information on FCs for the same data size. A reasonable scheme would also be to move all atoms as a superposition of the normal modes sampled from the canonical ensemble, if effective force constants at higher temperatures need to be extracted. If normal modes are not known, as is usually the case, one can still adopt normal modes generated with an arbitrary but cheap force field. This is done in the utility file `sc_snaps.x` which generates supercell snapshots of a required number if a temperature of interest is given. In principle, one or two snapshots in which all atoms are moved maybe sufficient to generate harmonic force constants. If only harmonic FCs are required, it is best to generate snapshots in which only one inequivalent atom is moved. More snapshots will be needed if anharmonic FCs are also required, typically on the order of 20, depending on their rank and chosen range. If the range of the required anharmonic FCs is increased, their number is also exponentially increased, and therefore more data (snapshots) would be needed to solve for all the unknowns. Checks must be performed to make sure the generated FCs don't change when the range is increased; just the furthest ones are added and are smaller than the existing ones. Another check for convergence is that the physical quantities of interest such as the phonon dispersion and the Gruneisen parameters do

not appreciably change as ranges are increased. Largest (infinite norm) and average (first norm) error, as well as the percentage deviation (second norm) on fitting are written at the end of the log file.

For Ge, we have used a supercell of 216 atoms with 36 snapshots in which only one or two atoms have been moved. Forces were calculated using VASP Kresse and Hafner (1993, 1994); Kresse and Furthmüller (1996a,b) with the GGA-PBESol functional, at cutoff energy of 225 eV and a Gamma-centered $7 \times 7 \times 7$ kpoint mesh within the $3 \times 3 \times 3$ supercell. The lattice constant of $a = 5.702 \text{ \AA}$ was found using $14 \times 14 \times 14$ kmesh for the primitive cell optimization calculations. This is only 0.7% larger than the experimental value of 5.66 Å. All harmonic FCs within the supercell were included in the fitting as shown in Fig. 2. Cubic force constants were included up to the 6th nearest neighbors. The results on the phonon dispersion and Gruneisen parameters are displayed in Fig. 3. The slight discrepancy between the computed and experimentally measured Nilsson and Nelin (1972) frequencies is most likely due to the larger PBE lattice constant of 5.7 Å, which is slightly larger than the experimental value of 5.66 Å. This is a 2.1% larger volume. Therefore for a Gruneisen parameter of +1 for instance, a 2.1% reduction in the phonon frequency should be expected. The Gruneisen parameters in Fig.3 show a very decent agreement with the values of Olego and Cardona Olego and Cardona (1982).

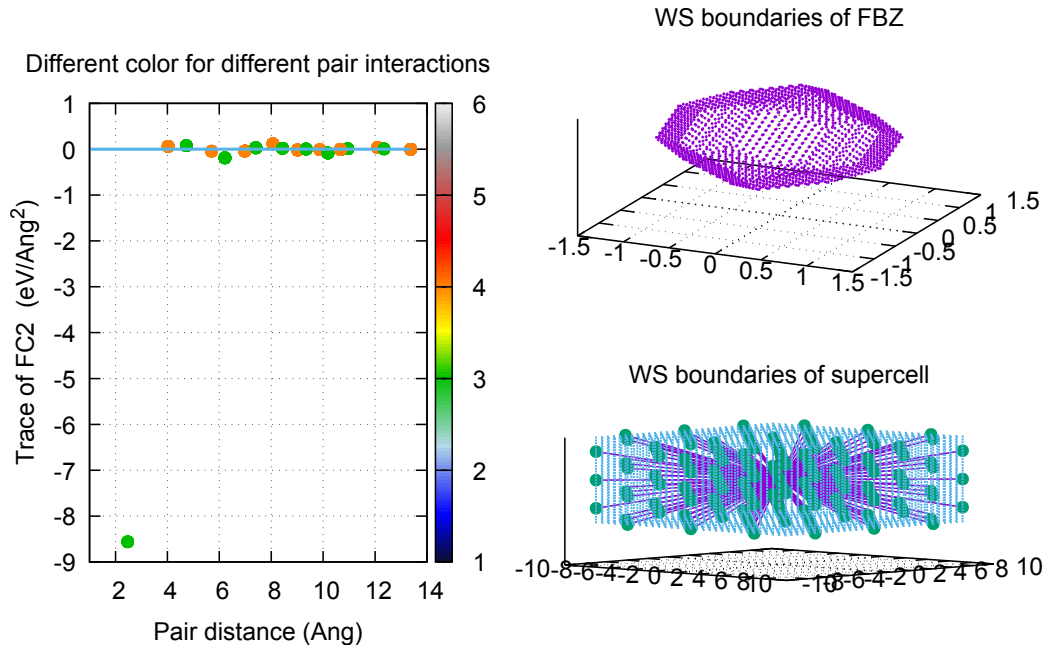


Figure 2: Output of the `fc.plt`: On the left are the fitted Ge harmonic force constants as a function of pair distance. Bottom right: To visualize included force constants, we show the Wigner-Seitz (WS) cell of the supercell (in blue) centered on an atom, the grid of primitive translation vectors (green spheres), and selected force constants (purple lines) connecting the central atom to its neighbors within the supercell. This can be visualized for every atom in the primitive cell. Top right: Wigner-Seitz cell of the Brillouin zone (purple dots).

To view the set of harmonic force constants used in the fitting, one can make a plot similar to Fig.2 by using the file `fcs.plt`.

The dispersion compares well with other available data. The elastic tensor is summarized in table 1. There is usually some fluctuation in the available data, depending on the temperature where measurements were taken, and on the numerical side, results depend on the lattice parameter and exchange-correlation functional used, and the method used to extract elastic constants.

For a crystal of cubic symmetry, the bulk B , Young Y and shear μ moduli are respectively given by: $B = (C_{11} + 2C_{12})/3$; $Y = 1/S_{11} = 3B(C_{11} - C_{12})/(C_{11} + C_{12})$; $\mu = C_{44}$; $\nu = -S_{12}/S_{11} = C_{12}/(C_{11} + C_{12})$. Note the expression for Y and ν assume deformation along the $[100]$ direction, and this is what we report in the table 1 below, in addition to their “isotropic” values, as defined in the previous section.

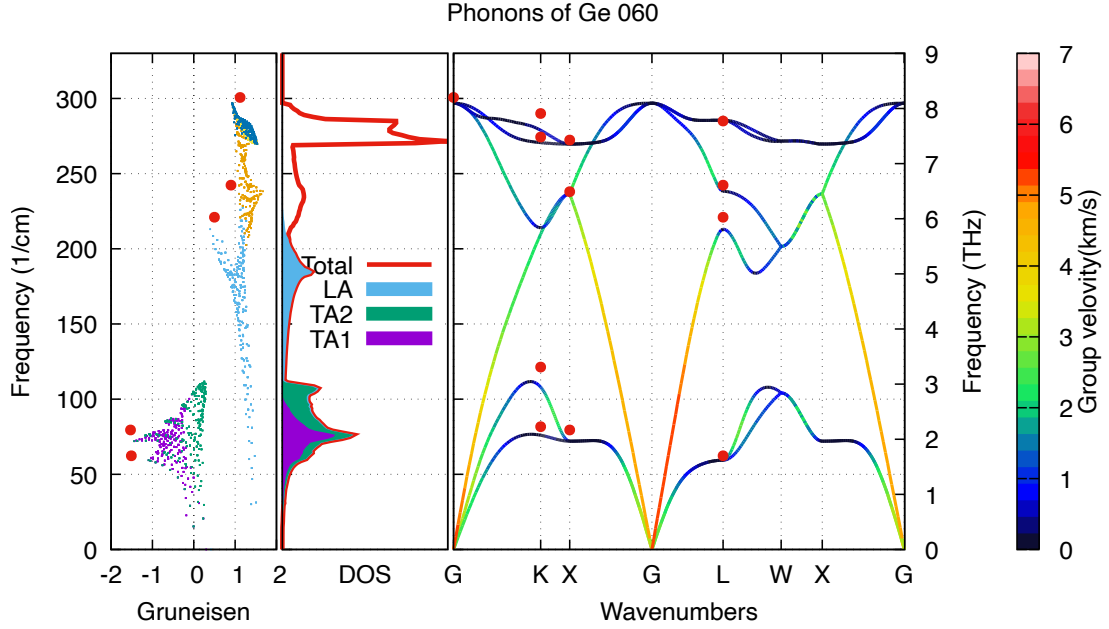


Figure 3: Mode Gruneisen parameters in the irreducible Brillouin zone (left), phonon density of states (center), and dispersion of Ge (right) calculated by FOCEX. Large red dots are experimental data. Color bar shows the group velocity magnitude in km/s

	C_{11}	C_{12}	C_{44}	B	Y_{100}	Y_{iso}	μ_{100}	μ_{iso}	v_{100}	v_{iso}
This work (LD model)	121	69	54.0	86.4	73	105	54	41	0.36	0.29
Experiment (Ioffe)	126	44	67.7	71.3		103		41		0.26
Experiment (McSkimin)	129	48.3	67.25	77	102.5		67.1			0.26
Materials Project (DFT)	102	36	56	58	83.3			47		0.25*

Table 1

Elastic constants of Ge crystal in GPa. Experimental data from McSkiminMcSkimin (1953) is at $T=298K$, and those of Ioffe Institute Database (????) are at $300K$. The reported value of 0.19 on MP is not consistent with $-S_{12}/S_{11} = 0.25$, but we are reporting the latter. For the Young and shear moduli and the Poisson ratio, we are reporting them for both deformations along $[100]$ and the average value denoted by the subscript *iso*.

Group velocities are also compared to the data in Ioffe siteDatabase (????). Results, which are presented in table 2, show relatively good agreement. It is worth noting that there is a simple relationship between group velocities near the zone center (sound speeds) and elastic constants in a cubic crystal. All 3 elastic constants can be extracted from the 3 speeds of sound along $[110]$:

$$\rho v_L^2(100) = C_{11} \quad \rho v_{T1}^2(100) = C_{44} \quad \rho v_{T2}^2(100) = C_{44} \quad (32)$$

$$\rho v_L^2(111) = \left(\frac{C_{11} + 2C_{12} + 4C_{44}}{3} \right) \quad \rho v_{T1}^2(111) = C_{44} \quad \rho v_{T2}^2(111) = \left(\frac{C_{11} - C_{12} + C_{44}}{3} \right) \quad (33)$$

$$\rho v_L^2(110) = \left(\frac{C_{11} + C_{12}}{2} + C_{44} \right) \quad \rho v_{T1}^2(110) = C_{44} \quad \rho v_{T2}^2(110) = \left(\frac{C_{11} - C_{12}}{2} \right) \quad (34)$$

Finally, we must add that this code has been used many times and its results validated in the past 15 years or so. The results on force constants or phonons and lattice thermal conductivity have been published as follows: SiliconEsfarjani, Chen, and Stokes (2011); Minnich, Johnson, Schmidt, Esfarjani, Dresselhaus, Nelson, and Chen (2011); Tian, Esfarjani, Shiomi, Henry, and Chen (2011); Scott, Hattar, Rost, Gaskins, Fazli, Ganski, Li, Bai, Wang,

Direction	[100]	[110]	[111]
This work (LD model)	3.44 4.76	2.77 3.78 5.11	3.26 5.43
Experiment (Ioffe)	3.57 4.87	2.77 3.57 5.36	3.06 5.51
Experiment (McSkimin)	3.54 4.91	2.75 3.55 5.41	- -

Table 2

Group velocities (km/s) of the three acoustic branches compared to experimental data from McSkimin (1953) and Ioffe (1953) taken at room temperature. The largest number corresponds to the longitudinal mode. Along [100] and [111] the two transverse acoustic branches are degenerate.

Esfarjani, Goorsky, and Hopkins (2018), half-Heuslers Shiomi, Esfarjani, and Chen (2011) FeSb₂ Liao, Lee, Esfarjani, and Chen (2014), graphene Mingo, Esfarjani, Broido, and Stewart (2010); Lee, Broido, Esfarjani, and Chen (2015), GaAs Maznev, Hofmann, Jandl, Esfarjani, Bulsara, Fitzgerald, Chen, and Nelson (2013), PbSe and PbTe Shiga, Shiomi, Ma, Delaire, Radzynski, Lusakowski, Esfarjani, and Chen (2012); Tian, Garg, Esfarjani, Shiga, Shiomi, and Chen (2012), Bi and Sb Lee et al. (2015).

Code availability

The Anharmonic Lattice Dynamics (ALADYN) suites of codes may be accessed and downloaded from <https://github.com/KeivanS/Anharmonic-lattice-dynamics>.

Documentation is available at:
<https://aladyn.readthedocs.io/en/latest/index.html>

Data availability

the data presented on Germanium, including inputs to FOCEX and all the generated output files can be accessed at: <https://doi.org/10.18130/V3/MVKFQ7>

8. Acknowledgements

Financial support of SNS, YL, BT, RS and KE by NSF-CSSI award #2103989 are gratefully acknowledged.

References

- K. Esfarjani, H. T. Stokes, Method to extract anharmonic force constants from first principles calculations, *Phys. Rev. B* 77 (2008) 144112.
- T. Tadano, Y. Gohda, S. Tsuneyuki, Anharmonic force constants extracted from first-principles molecular dynamics: Applications to heat transfer simulations, *Journal of Physics Condensed Matter* 26 (2014) 225402.
- T. Tadano, S. Tsuneyuki, First-principles lattice dynamics method for strongly anharmonic crystals, *Journal of the Physical Society of Japan* 87 (2018) 041015.
- W. Li, J. Carrete, N. A. Katcho, N. Mingo, ShengBTE: a solver of the Boltzmann transport equation for phonons, *Comp. Phys. Commun.* 185 (2014) 1747–1758.
- J. Carrete, B. Vermeersch, A. Katre, A. van Roekeghem, T. Wang, N. Madsen, Georg K. H. and Mingo, almbte : A solver of the space–time dependent Boltzmann transport equation for phonons in structured materials, *Computer Physics Communications* 185 (2017) 1747.
- A. Togo, I. Tanaka, First principles phonon calculations in materials science, *Scripta Materialia* 108 (2015) 1 – 5.
- L. Monacelli, R. Bianco, M. Cherubini, M. Calandra, I. Errea, F. Mauri, The stochastic self-consistent harmonic approximation: calculating vibrational properties of materials with full quantum and anharmonic effects, *Journal of Physics: Condensed Matter* 33 (2021) 363001.
- F. Eriksson, E. Fransson, P. Erhart, The hiphive package for the extraction of high-order force constants by machine learning, *Advanced Theory and Simulations* 2 (2019) 1800184.
- O. Hellman, P. Steneteg, I. A. Abrikosov, S. I. Simak, Temperature dependent effective potential method for accurate free energy calculations of solids, *Phys. Rev. B* 87 (2013) 104111.
- O. Hellman, I. A. Abrikosov, Temperature-dependent effective third-order interatomic force constants from first principles, *Phys. Rev. B* 88 (2013) 144301.
- K. Parlinski, Z. Q. Li, Y. Kawazoe, First-principles determination of the soft mode in cubic ZrO₂, *Phys. Rev. Lett.* 78 (1997) 4063–4066.
- D. Alfè, PHON: A program to calculate phonons using the small displacement method, *Computer Physics Communications* 180 (2009) 2622–2633.
- G. Liebfried, W. Ludwig, *Solid State Physics*, volume 12, Academic, 1961.
- M. Born, K. Huang, *Dynamical Theory of Crystal Lattices*, Oxford University Press, Oxford, England, 1954.
- M. Sluiter, M. Weinert, Y. Kawazoe, Determination of the elastic tensor in low-symmetry structures, *EPL (Europhysics Letters)* 43 (1998) 183.

- M. H. Sluiter, M. Weinert, Y. Kawazoe, Force constants for substitutional alloys, *Physical Review B* 59 (1999) 4100.
- A. A. Maradudin, A. E. Fein, Scattering of neutrons by an anharmonic crystal, *Phys. Rev.* 128 (1962) 2589–2608.
- X. Gonze, C. Lee, Dynamical matrices, born effective charges, dielectric permittivity tensors, and interatomic force constants from density-functional perturbation theory, *Physical Review B - Condensed Matter and Materials Physics* 55 (1997) 10355–10368.
- S. Baroni, S. de Gironcoli, A. Dal Corso, P. Giannozzi, Phonons and related crystal properties from density-functional perturbation theory, *Rev. Mod. Phys.* 73 (2001) 515–562.
- P. P. Ewald, The calculation of optical and electrostatic grid potential, *Ann. Phys. (Leipzig)* 64 (1921) 253.
- K. Ohno, K. Esfarjani, Y. Kawazoe, *Computational materials science: From Ab Initio to Monte Carlo methods*, 2nd ed., Springer Series in Solid-State Sciences, Berlin Heidelberg, 2018. doi:10.1007/9783662565421.
- A. Togo, L. Chaput, T. Tadano, I. Tanaka, Implementation strategies in phonopy and phono3py, *Journal of Physics: Condensed Matter* 35 (2023) 353001.
- D. Wallace, *Thermodynamics of Crystals*, John Wiley and Sons, Inc., Dover, Mineola, New York, 1998.
- N. R. Werthamer, Self-consistent phonon formulation of anharmonic lattice dynamics, *Physical Review B* 1 (1970) 572–581.
- K. Esfarjani, Y. Liang, Thermodynamics of anharmonic lattices from first principles, in: *Nanoscale Energy Transport*, 2053-2563, IOP Publishing, 2020, pp. 7–1 to 7–35. URL: <https://dx.doi.org/10.1088/978-0-7503-1738-2ch7>. doi:10.1088/978-0-7503-1738-2ch7.
- K. Esfarjani, Y. Liang, Equilibrium and non-equilibrium lattice dynamics of anharmonic systems, *Entropy* 24 (2022) 1585.
- G. Kresse, J. Hafner, *Phys. Rev. B* 47 (1993) 558.
- G. Kresse, J. Hafner, *Phys. Rev. B* 49 (1994) 14251.
- G. Kresse, J. Furthmüller, *Comput. Mat. Sci.* 6 (1996a) 15.
- G. Kresse, J. Furthmüller, Efficient iterative schemes for ab initio total-energy calculations using a plane-wave basis set, *Phys. Rev. B* 54 (1996b) 11169–11186.
- G. Nilsson, G. Nelin, Study of the homology between silicon and germanium by thermal-neutron spectrometry, *Phys. Rev. B* 6 (1972) 3777–3786.
- D. Olego, M. Cardona, Pressure dependence of raman phonons of ge and 3c-sic, *Phys. Rev. B* 25 (1982) 1151–1160.
- H. McSkimin, Measurement of elastic constants at low temperatures by means of ultrasonic waves—data for silicon and germanium single crystals, and for fused silica, *J. Appl. Phys.* 24 (1953) 988.
- I. I. Database, Ge semiconductor data from the ioffe institute website, ??? URL: <https://www.ioffe.ru/SVA/NSM/Semicond/Ge/>.
- K. Esfarjani, G. Chen, H. T. Stokes, Heat transport in silicon from first-principles calculations, *Phys. Rev. B* 84 (2011) 085204.
- A. J. Minnich, J. A. Johnson, A. J. Schmidt, K. Esfarjani, M. S. Dresselhaus, K. A. Nelson, G. Chen, Thermal conductivity spectroscopy technique to measure phonon mean free paths, *Phys. Rev. Lett.* 107 (2011) 095901.
- Z. Tian, K. Esfarjani, J. Shiomi, A. S. Henry, G. Chen, On the importance of optical phonons to thermal conductivity in nanostructures, *Applied Physics Letters* 99 (2011) 053122.
- E. A. Scott, K. Hattar, C. M. Rost, J. T. Gaskins, M. Fazli, C. Ganski, C. Li, T. Bai, Y. Wang, K. Esfarjani, M. Goorsky, P. E. Hopkins, Phonon scattering effects from point and extended defects on thermal conductivity studied via ion irradiation of crystals with self-impurities, *Phys. Rev. Mater.* 2 (2018) 095001.
- J. Shiomi, K. Esfarjani, G. Chen, Thermal conductivity of half-Heusler compounds from first-principles calculations, *Physical Review B - Condensed Matter and Materials Physics* 84 (2011) 104302.
- B. Liao, S. Lee, K. Esfarjani, G. Chen, First-principles study of thermal transport in fcs 2, *Physical Review B - Condensed Matter and Materials Physics* 89 (2014) 035108.
- N. Mingo, K. Esfarjani, D. A. Broido, D. A. Stewart, Cluster scattering effects on phonon conduction in graphene, *Physical Review B - Condensed Matter and Materials Physics* 81 (2010) 1–6.
- S. Lee, D. Broido, K. Esfarjani, G. Chen, Hydrodynamic phonon transport in suspended graphene, *Nature Communications* 6 (2015) 6290.
- A. A. Maznev, F. Hofmann, A. Jandl, K. Esfarjani, M. T. Bulsara, E. A. Fitzgerald, G. Chen, K. A. Nelson, Lifetime of sub-thz coherent acoustic phonons in a GaAs-AlAs superlattice, *Applied Physics Letters* 102 (2013).
- T. Shiga, J. Shiomi, J. Ma, O. Delaire, T. Radzynski, A. Lusakowski, K. Esfarjani, G. Chen, Microscopic mechanism of low thermal conductivity in lead telluride, *Physical Review B - Condensed Matter and Materials Physics* 85 (2012) 155203.
- Z. Tian, J. Garg, K. Esfarjani, T. Shiga, J. Shiomi, G. Chen, Phonon conduction in PbSe, PbTe, and PbTe 1-xSe x from first-principles calculations, *Physical Review B - Condensed Matter and Materials Physics* 85 (2012) 184303.